International Journal of Rotating Machinery, 9: 239–246, 2003

ISSN: 1023-621X
DOI: 10.1080/10236210390202667

Reduction of Discrete-Frequency Fan Noise Using Slitlike Expansion Chambers

Akira Sadamoto and Yoshinori Murakami
Department of Mechanical Engineering, Tsukuba College of Technology, Tsukuba, Ibaraki, Japan

As is generally known, discrete-frequency noises are radiated from fans due to rotor-stator interaction. Their fundamental frequency is the blade-passage frequency, which is determined by the number of rotor blades and their rotating speeds. To reduce such noises, several types of silencers have been designed. Among them, the authors noted a slitlike expansion chamber (hereafter referred to as *slit*, for simplicity) and have studied its performance. A slit is a simple expansion chamber with a very short axial length that is placed in a duct. A slit with a circular cross-section that is concentric with a circular duct may be studied using the same interpretation as is used for a side-branch resonator muffler (a closed-end tube connected to a duct); that is, the resonant frequency of a slit depends on its depth (with an open-end correction). It is expected, hence, that a slit might be applicable as a simple and axially compact silencer that is effective on discrete-frequency noises. In this article, the properties of a slit are introduced, and the applicability of a slit to actual rotating machinery is described using experimental data.

Keywords Discrete-frequency noise, Expansion chamber, Fan noise, Noise reduction, Rotor-stator interaction, Slit

An expansion chamber in a duct is well known to be a sound attenuator. Generally, in order to obtain the effect of noise reduction in the low-frequency range, the chamber must have a long axial length relative to its diameter (e.g., El-Sharkawy and Nayfeh, 1978). Some researchers (e.g., Ih and Lee, 1985), however, have investigated the properties of a short chamber that acts as a resonator muffler when its length becomes shorter than a specific value. We noticed this property and thought to construct a compact silencer that could be realized if the property were maintained so that the chamber length became very short. So we investigated the properties of a very short expansion chamber experimentally and analytically (Sadamoto et al., 1993; Sadamoto and Murakami, 1998).

A very short expansion chamber resembles a slit groove on the inner wall of a duct, so we called it a slit. The advantages of a slit as a silencer were expected to be as follows: it has a simple shape and is easy to construct; it is very short in the axial direction and is easy to put into a narrow axial space, for example, into connecting pipes (between two flanges opposed to each other) or onto an inlet of fluid; and the influence of such a silencer on fluid flow is smaller than that of other types of mufflers.

To exploit these advantages, the actual performance of slits had to be confirmed experimentally in cases in which slits were applied to actual machinery. For this reason, we examined two cases: (1) a slit was applied to a centrifugal-flow fan motor (blower) for a home-use vacuum cleaner as an example of a relatively small-diameter case; and (2) it was applied to a laboratory-use axial flow wind tunnel as an example of a considerably large-diameter case. The results of these two cases are the main fruits of this paper.

PERFORMANCE OF SLITS

In this section, the properties of slits are summarized.

As shown in Figure 1, in an axially infinite circular duct with diameter D, a single short circular expansion with diameter d and length l is located concentric to the duct. The slit depth b is also an important parameter, which is given by $(d–D)/2$. In this section, the performance of this expansion is shown using the transmission coefficient that is defined as the value of the transmitted wave's absolute amplitude divided by the incident wave's

Received 25 June 2002; accepted 1 July 2002.
A portion of this research was supported by the Japan Society for the Promotion of Science through the Grant-in-Aid for Encouragement of Young Scientists (No. 10750132).
We also express our thanks to our colleague Dr. T. Tani for his help with our experiment.
Address correspondence to Akira Sadamoto, Department of Mechanical Engineering, Tsukuba College of Technology, 4-3 Amakubo, Tsukuba, Ibaraki, 305-0005 Japan. E-mail: sada@a.tsukuba-tech.ac.jp

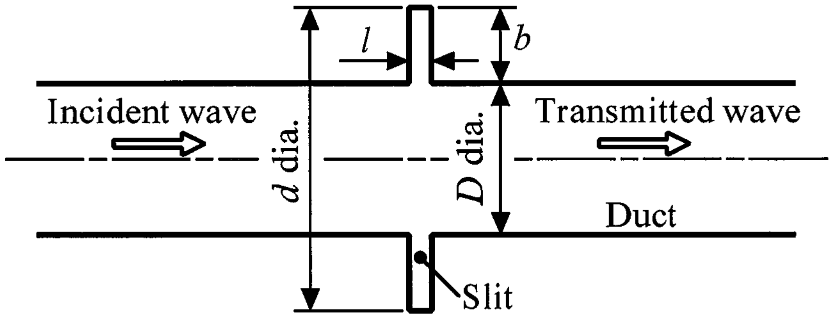

FIGURE 1
A slit in a circular duct.

absolute amplitude. In this section we discuss the plane wave only. We examined several cases, including cases of higher-order modes (Sadamoto and Murakami, 2002), but we omit those data here so as to show the basic character of the slit.

As some researchers (e.g., Sullivan and Crocker, 1978) have pointed out, a chamber becomes a resonant chamber when $l/d < 0.41$. In addition, based on the results of our research (see Sadamoto and Murakami, 2002), it can be said that a chamber becomes a slit-type chamber when $l/d < 0.1$, where *slit-type* means that the chamber acts as a side-branch type of silencer; this property is realized by the interaction of sounds in the branch axis direction. In other words, the slit acts as a closed-end tube connected to the duct, and the resonant frequency is obtained when a quarter of the incident sound's wavelength becomes equal to the length of the tube with an open-end correction.

In order to indicate the slit property briefly, some examples of measured transmission coefficients are shown in Figure 3; they were obtained using the apparatus in Figure 2, which contained 25°C air. In this apparatus, a plane wave with an arbitrary monotonic frequency f was generated in a 41.3-mm-diameter pipe, using the speaker. Then it was received by the microphone, and the absolute amplitude of the sound pressure was measured in the following two cases: the slit with diameter d and length l was located between the speaker and the microphone; the slit was replaced by the ring with diameter D and length l, that is, the pipe became uniform between the speaker and the microphone. The former amplitude divided by the latter one gives the transmission coefficient at the slit.

As is evident in Figure 3, the slit actually performs as a resonator muffler. In the extremely short cases, however, the minimum transmission coefficients do not reach zero. Their value becomes larger as l becomes shorter. This is caused by the insufficient resonance in the slit, which occurs because the influence of the viscous damping at the inlet and outlet walls of the expansion becomes too great to be neglected (see Sadamoto and Murakami, 1998). In our experience, this influence becomes negligible when $l \geq 5$ mm.

In Figure 3, the curved lines are added to indicate the calculated transmission coefficients obtained using our analytical method (see Sadamoto and Murakami, 2002). This method was developed on the basis of the traditional calculation methods (Alfredson, 1972; Miles, 1944), which are as follows. Using the equation of sound pressure in a duct including higher-order modes, simultaneous equations are conducted to solve complex

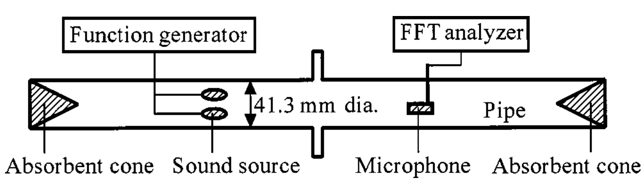

FIGURE 2
Experimental apparatus to measure transmission properties of the slit.

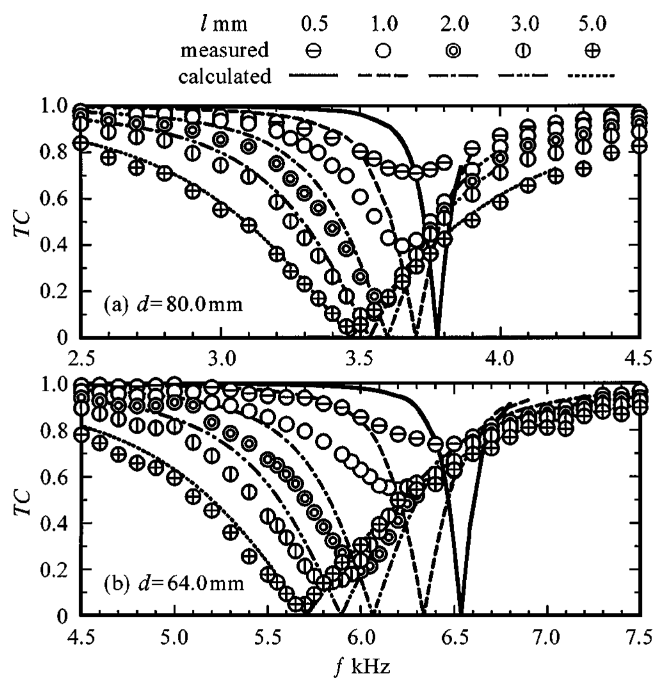

FIGURE 3
Transmission coefficient at the slit: the plane wave incidence, $D = 41.3$ mm.

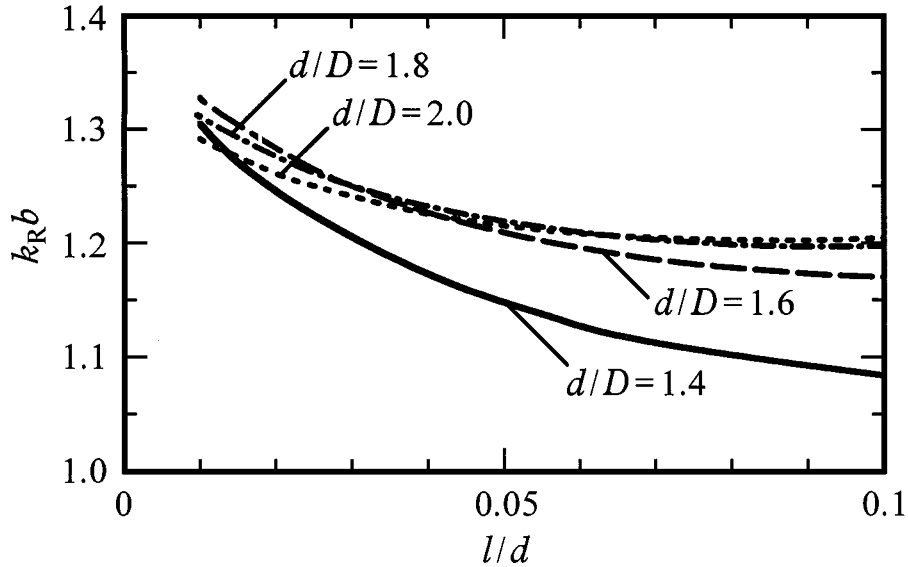

FIGURE 4
Calculated resonant frequency of the slit normalized by the slit depth.

amplitudes of reflected and transmitted waves for an incident wave at an abrupt expansion or reduction in a duct. Considering each calculated wave's axial propagation (or attenuation, for nonpropagating modes) in an expansion, calculations of reflection and transmission are repeated many times at both ends of the expansion; this procedure is finished when summations of them converge.

Because this method does not take the viscous damping into account, each curve reaches zero at each resonant frequency, even when the slit length is extremely short. In cases of $l \leq$ 3 mm, the difference between the calculated and the measured resonant frequency becomes greater as l becomes shorter (in the measured data, the resonant frequency was obtained where the transmission coefficient became minimum). However, this difference is not serious, and we judged that the resonant frequency could be properly predicted using our calculation.

For reference, the calculated resonant frequencies are summarized in Figure 4, where the nondimensional parameters are used (see Sadamoto and Murakami, 2002); that is, the resonant frequency is normalized by the slit depth as the product of the planar wave number at the resonance k_R and the slit depth b, and the size of the duct and the slit are normalized as d/D and l/d. In this figure, $k_R b$ becomes about 1.3 as l/d reaches zero, regardless of d/D. This value of 1.3 is about 17% less than $\pi/2$; 17% corresponds to an open-end correction from the viewpoint of a side branch that obeys k_R[(branch depth) + (open-end correction)] $= \pi/2$.

APPLICATION OF SLITS TO THE OPEN END OF A SMALL DUCT

In this section, as an example of a relatively small open end in rotating machinery, a fan motor for a home-use vacuum cleaner was used to study a slit on its inlet that had a 37-mm diameter.

In Figure 5, the layout of the apparatus is shown. The fan motor was supported horizontally at a height of 1 m from the laboratory's floor. The laboratory was not equipped with anechoic facings, but the room was large enough and the sound frequency of interest was sufficiently high that the measurement was likely to be a reliable representation of the actual performance of the slit. At the inlet of this fan motor, a short pipe was mounted in order to attach the ring that forms the slit, as shown in Figure 6. At a point .50 m away from this ring end, a condenser microphone with a $^1/_2$-in diameter was located. The frequency response of this microphone was rated flat from 20 Hz to 12.5 kHz, as certified by the Japanese Industrial Standard. The received sound pressure was recorded by the Digital Audio Tape (DAT) recorder and analyzed using the Fast Fourier Transform (FFT) analyzer. The spectrum was calculated in the range below 10 kHz, with a 25-Hz resolution and a Hanning window. The rotating speed of the fan motor was

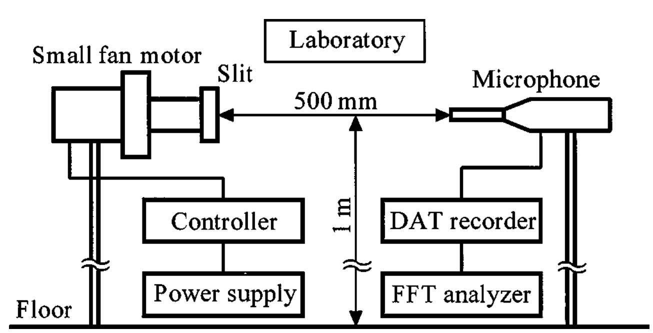

FIGURE 5
Apparatus to measure noise radiated from the small fan motor.

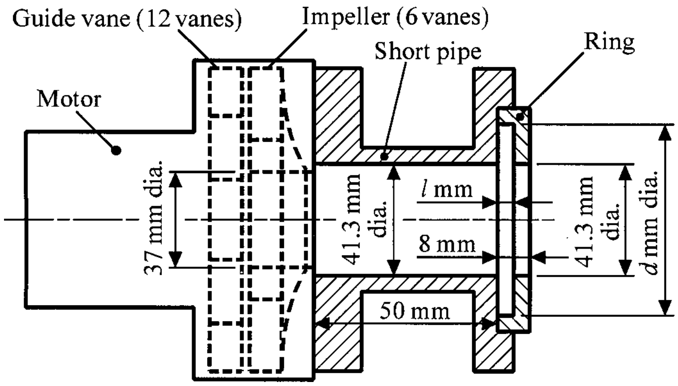

FIGURE 6
Placement of the slit attached to the small fan motor.

easy to control by changing the voltage going to the motor; that is, the frequency of the discrete-frequency noises was easy to control.

As shown in Figure 6, the slit was formed using a ring, which has a hollow in one side with diameter d and length l and was clamped to the end of the short pipe. In cases in which no slit was required, a ring with no hollow but of the same thickness was used instead.

In Figure 7, the spectrum of the noise radiating from the fan motor with the short pipe is shown. In the case with no slit ($l = 0$), the discrete-frequency noises are observed at 1.8 kHz and 3.6 kHz. These frequencies are easily seen to be multiples of the blade-passage frequency (e.g., Tyler and Sofrin, 1961), which can be calculated by

$$f_{\mathrm{B}} = n \cdot n_{\mathrm{B}} N \qquad [1]$$

where n is an arbitrary positive integer, n_{B} is the number of the rotor blades, and N is the rotating speed. In the case of Figure 7, N was fixed at 300 Hz (18,000 rpm) and n_{B} was 6, as shown

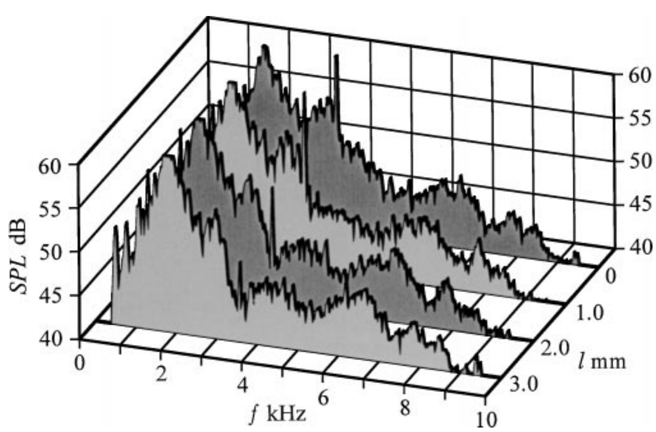

FIGURE 7
Spectrum of the noise radiated from the inlet of the small fan motor: without a slit ($l = 0$); with a slit ($D = 41.3$ mm, $d = 80.0$ mm).

in Figure 6. These conditions yield $f_{\mathrm{B}} = 1800 \cdot n$ Hz in Equation (1). Then f_{B} becomes 1.8 kHz for $n = 1$ and 3.6 kHz for $n = 2$. When these two peaks at these frequencies are compared, the latter one looks more conspicuous in view of the difference in level between it and the noise in the ambient frequency range. This peak was, hence, chosen as a target so as to reduce the use of the slit.

As shown in Figure 3, the slit with $d = 80$ mm in a duct with $D = 41.3$ mm is expected to be effective near 3.6 kHz, so in order to reduce the target peak, this slit diameter (80 mm) was used with several lengths l.

Figure 7 shows that the slit actually is effective for reducing the 3.6-kHz peak. In addition, it is also clear that the peak decreases as l becomes longer. This is recognized by making the same interpretation as is shown in Figure 3—the influence of the insufficient resonance in extremely short slits.

As a quantitative estimate, the transmission loss by the slit with $l = 3$ mm is shown in Figure 8, which indicates the difference between two spectrums ($l = 3$ and 0 mm). The maximum attenuation is obtained at about 15 dB near 3.6 kHz, which is the same level expected under the circumstances shown in Figure 3. Although the configurations differ considerably in Figure 2 (the duct length is infinite, as an ideal case) and Figure 6 (the slit is located very close to an open end, as an actual case), the performance of the slit becomes similar in both cases. It is also remarkable that the level of the spectrum is not changed in the frequency range except near the target frequency. As a result, the slit is expected to be a sound attenuator applicable to discrete-frequency noises without any adverse effect on other frequency ranges.

APPLICATION OF SLITS TO THE OPEN END OF A LARGE DUCT

To study a considerably large open end in a piece of rotating machinery, the laboratory's wind tunnel was used to apply the slit to the inlet that was 708 mm in diameter.

In Figure 9, the layout of the apparatus is shown. Because the inlet of the wind tunnel, which is located in the laboratory, is close to the wall of the building, the microphone was located outdoors. The sound was radiated through a rectangular opening, in the wall of which each side length was about 0.9 m. The measurement was carried out on a day with no wind and sufficiently suppressed surrounding noise. Since the outer field of the building is wide and there are some trees, it was reasonable to suppose that the field was anechoic. The rotating speed of the rotor (rotor speed) could be precisely adjusted using the transmission, and it was measured using an optically sensed tachometer. The equipment for analysis of the sound (microphone, etc.) were the same as that mentioned in the previous section.

The slit was formed, as shown in Figure 10, by two rings that were clamped onto the flange at the end of the wind tunnel. Ordinarily, a short, bell-mouth–shaped duct is connected there, but it was removed for the experiment. In order to form the end with no slit, the slit ring (1108 mm in diameter) was simply

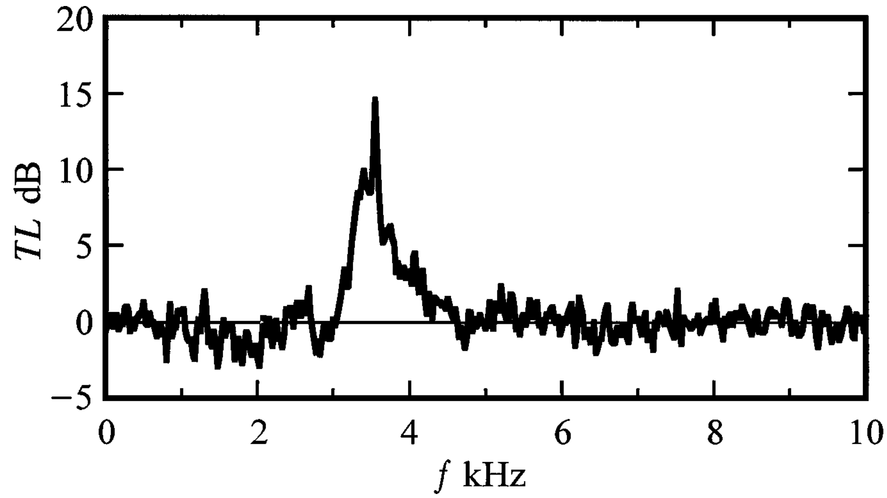

FIGURE 8
Effect of the slit attached to the small fan motor: $D = 41.3$ mm, $d = 80.0$ mm, and $l = 3.0$ mm.

removed. That meant that the axial lengths of the two ends were slightly different. In this situation, the effect of inserting the slit was estimated. Even so, on account of the slit length l that was too short compared with the duct diameter, it was supposed that there would be almost no difference between that case and the case in which the duct length was correctly adjusted, as shown in Figure 6.

In order to know the character of the wind-tunnel noise, the sound was measured with no slit, varying the rotor speed within an appropriate range. An example of these results is shown in Figure 11, where it is obvious that some peaks appear in the broadband noise, whose level becomes smaller as the frequency becomes higher. Although this broadband noise level increased as the rotor speed (the flow speed in the wind tunnel) increased, it was not serious relative to the peak level under the conditions of this research.

The peaks indicated by (B) in Figure 11 were found to remain unchanged when the rotor speed was changed (to avoid confusion, only two rotor speeds are presented). In fact, we measured several spectrums at many other rotor speeds and confirmed that the frequencies of these peaks never change. They were caused by the noise radiated from the driveline of the wind tunnel and were extraneous to our interest in this research, as they could not be reduced by the slit.

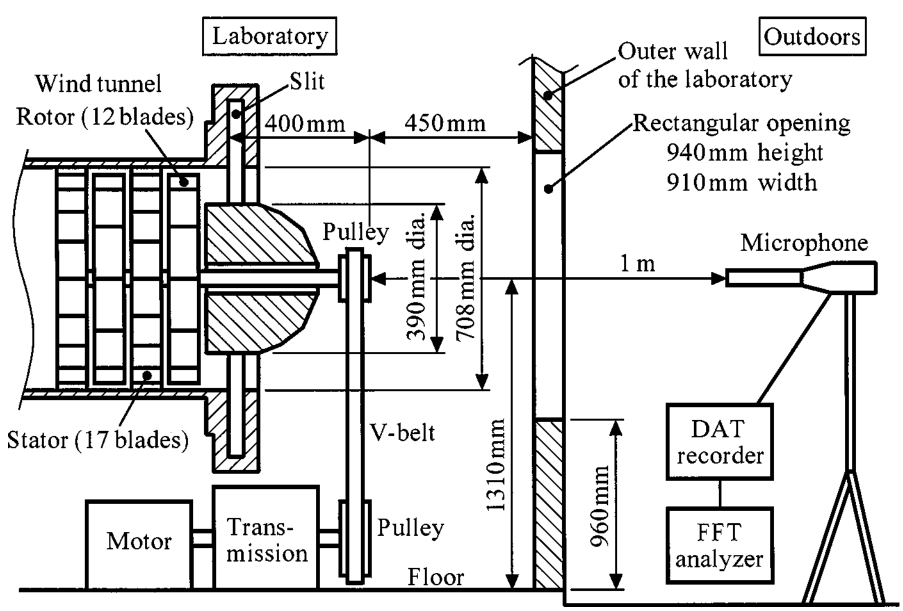

FIGURE 9
Apparatus to measure noise radiated from the inlet of the wind tunnel.

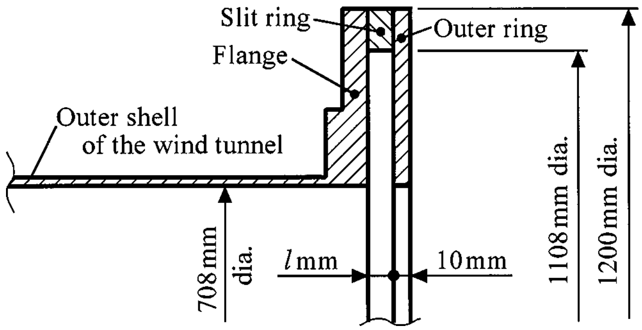

FIGURE 10
Formation of the slit on the inlet of the wind tunnel.

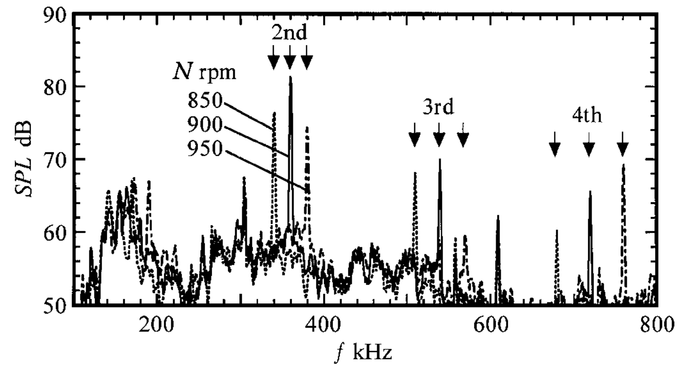

FIGURE 12
Spectrum of the noise radiated from the inlet of the wind tunnel in the frequency range of interest.

On the other hand, the peaks indicated by (A) in Figure 11 were found to change with the rotor speed, and they seemed to depend on the rotor-stator interaction. In order to understand these peaks, spectrums in the low-frequency range were studied, with 1.35-Hz resolution, as shown in Figure 12. The largest peak in this figure was obtained at 360 Hz and a rotor speed of $N =$ 900 rpm, which can be easily calculated, using Equation (1), to be twice the blade-passage frequency, that is, $f_P = 2 \cdot 12 \cdot (900/60)$. We examined various rotor speeds and confirmed that the second, third, and fourth components of the blade-passage frequency were observed in many cases, as shown in Figure 12. These peaks' levels were large compared with the ambient noise level. In addition, in many cases of each rotor speed, it was found that the second one was larger than the others by about 10 dB or more. Hence, this peak was chosen as the target peak.

In Figure 12, each second peak appears at around 360 Hz, in accordance with the rotor speed (around 900 rpm). As shown in Figure 4, the resonant frequency of a slit is obtained at $k_R b \approx 1.3$. According to this value, b becomes $1.3/k_R = 1.3/(2\pi f/c) = 1.3/(2\pi \cdot 360) \cdot 347 = 0.197$ m in the present case, where $c = 347$ m/sec is the sound speed in a free space at 25°C, which corresponds to the ambient temperature in the experiment. Consequently, the slit depth b was chosen to be 200 mm, and this is the reason that d is 1108 mm, as shown in Figure 10. On the other hand, to clarify the effect of the slit length, slit rings with $l = 10$, 20, and 30 mm were prepared. In addition, the rotor speed was gradually changed, as shown in Table 1, where the second blade-passage frequencies are also indicated.

In order to indicate the effect of the slit, some examples of the measured spectrums are shown in Figure 13; the rotor speed was fixed at 925 rpm and the corresponding second peak appeared at 370 Hz. It is obvious from these figures that the target peak (370 Hz) was suppressed in each case, and the attenuation level became larger as l became longer; it became almost 20 dB using the slit with $l = 30$ mm. In addition, it should be pointed out that the noise level at all frequencies except the target frequency was almost unchanged, regardless of the existence of the slit.

In fact, we measured each spectrum at each rotor speed shown in Table 1. For each speed, the spectrums measured in the cases

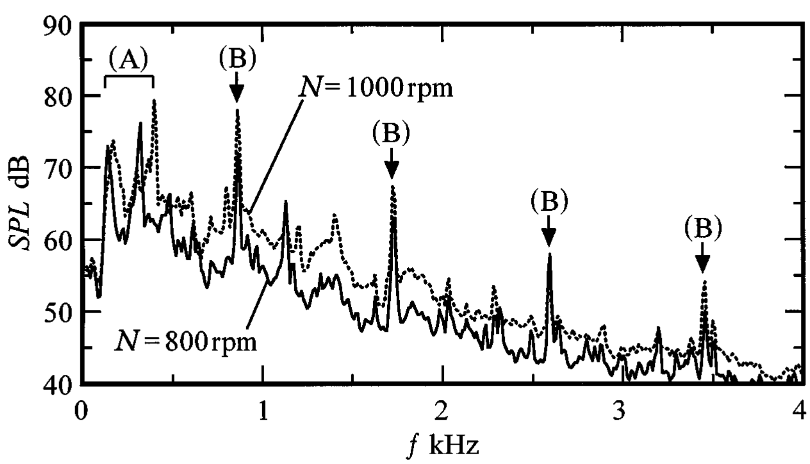

FIGURE 11
Spectrum of the noise radiated from the wind tunnel. (A) Peaks caused by rotor-stator interaction. (B) Peaks radiated from the driveline of the wind tunnel.

TABLE 1
Settings of the Rotor Speed for the Measurement

N rpm	850	863	875	888	900	913	925	938	950
f_B Hz (2nd)	340	345	350	355	360	365	370	375	380

in which the slit was $l = 10$, 20, and 30 mm were compared to the spectrums in cases without the slit. In many cases, the attenuation of the target peak was confirmed, and in all cases except the target peak, the noise level was almost unchanged, regardless of the presence of the slit.

The attenuation level (insertion loss) of the target peak for each case is indicated in Figure 14. The frequency indicated in the transverse axis of this graph corresponds to each peak

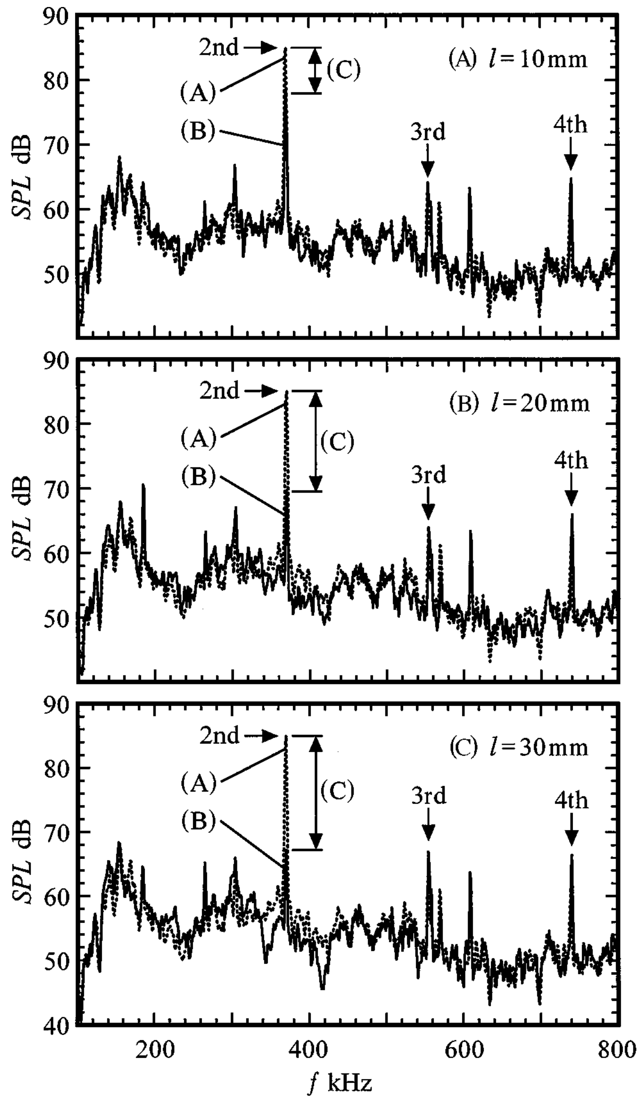

FIGURE 13
Spectrum of the noise radiated from the inlet of the wind tunnel driven at 925 rpm. (A) Without a slit. (B) With a slit (length l). (C) The effect of a slit.

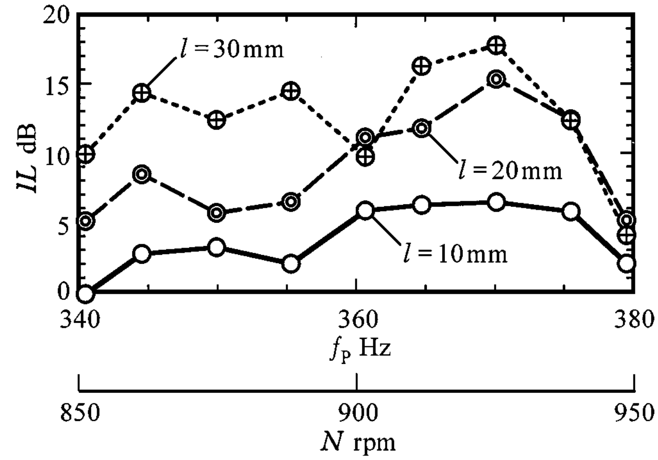

FIGURE 14
Effects of the slit with length l to the target peak at f_P of the noise radiated from the inlet of the wind tunnel driven at each speed N.

frequency f_P that was obtained at each driving speed N. In the cases of $l = 20$ and 30 mm, the largest attenuation level became about 15 dB or more, which seemed to be sufficient in view of the noise reduction. Although the maximum effectiveness of the slit with $l = 20$ mm was not so different from the one with $l = 30$ mm, the effective frequency range seemed to be wider in the case of $l = 30$ mm than in the case of $l = 20$ mm. This tendency was indicated by our calculation results (e.g., Figure 3), in which the effective frequency range became wider as the slit length became longer. On the other hand, in the case of $l = 10$ mm, the largest attenuation level was about 7 dB, which was considerably smaller than in the cases in which $l = 20$ or 30 mm. In spite of our expectation that the influence of the viscous damping on the slit wall would be negligible in the case of $l = 10$ mm, this length might not be enough to achieve sufficient resonance in the case of the large duct treated here.

As mentioned earlier, it was revealed that the slit performed as a compact muffler of discrete-frequency noises radiated from the large-duct inlet. In addition, although the wind tunnel had a dome-shaped nose in its inlet, as shown in Figure 9, and the sound field at the inlet was not circular but annular, the effective frequency of the slit in its inlet was properly predicted by using our calculation result for an ideal circular duct case (Figure 4).

CONCLUSION

In this article, some examples of the properties of a slitlike expansion chamber used as a resonator muffler have been introduced for an ideal case (a slit in an infinite-length duct). Then the performance of the slit in reducing discrete-frequency noises radiated from one end of a piece of rotating machinery was indicated experimentally by two cases: a small-diameter case using a small fan motor, and a large-diameter case using a wind tunnel. In both cases, the slit performed well as a silencer. It was found that the effective frequency of the slit in each case was properly predicted by our calculations, and the reduction level of the target peak was sufficient except in the case in which the extremely short slit was used. Consequently, as a simple and axially compact muffler of discrete-frequency noises, the slit is applicable to actual rotating machinery.

NOMENCLATURE

b	Slit depth
c	Speed of sound in free space
d	Slit diameter
D	Diameter of duct or inlet
f	Frequency
IL	Insertion loss
k	Wave number
l	Axial length of slit
n	Positive integer
N	Rotating speed of machinery
SPL	Sound pressure level
TC	Transmission coefficient
TL	Transmission loss
π	Circular constant

Subscripts

B	Blade
P	Peak
R	Resonance

REFERENCES

Alfredson, R. J. 1972. The propagation of sound in a circular duct of continuously varying cross-sectional area. *Journal of Sound and Vibration* 23:433–442.

El-Sharkawy, A. I., and Nayfeh, A. H. 1978. Effect of an expansion chamber on the propagation of sound in circular ducts. *Journal of the Acoustical Society of America* 63:667–674.

Ih, J., and Lee, B. 1985. Analysis of higher-order mode effects in the circular expansion chamber with mean flow. *Journal of the Acoustical Society of America* 77:1377–1388.

Miles, J. 1944. The reflection of sound due to a change in cross section of a circular tube. *Journal of the Acoustical Society of America* 16:14–19.

Sadamoto, A., Murakami, Y., and Masuda, S. 1993. Attenuation of sound including higher-order mode waves in circular duct using a narrow slit on the duct wall. *Transactions of the Japan Society of Mechanical Engineers (Series C)*. 59:3860–3865. [In Japanese.]

Sadamoto, A., and Murakami, Y. 1998. Quantitative estimate of sound attenuation of a slit-like duct expansion considering sound damping in it. *Transactions of the Japan Society of Mechanical Engineers (Series C)*. 64:1985–1990. [In Japanese.]

Sadamoto, A., and Murakami, Y. 2002. Resonant properties of short expansion chambers in a circular duct: including extremely short cases and asymmetric mode wave incidence cases. *Journal of Sound and Vibration* 249:165–187.

Sullivan, J. W., and Crocker, M. J. 1978. Analysis of concentric-tube resonators having unpartitioned cavities. *Journal of the Acoustical Society of America* 64:207–215.

Tyler, J. M., and Sofrin, T. G. 1961. Axial flow compressor noise studies. *S.A.E. Transaction* 70:309–332.